Backside observation of large-scale integrated circuits with multilayered interconnections using laser terahertz emission microscope

Masatsugu Yamashita,[1,a)] Chiko Otani,[1] Kodo Kawase,[1,2] Toru Matsumoto,[3] Kiyoshi Nikawa,[4] Sunmi Kim,[5] Hironaru Murakami,[5] and Masayoshi Tonouchi[5]
[1]*RIKEN, 519-1399 Aoba, Aramaki, Aoba-ku, Sendai, Miyagi 980-845, Japan*
[2]*Nagoya University, Furocho, Chikusa, Nagoya 464-8603, Japan*
[3]*Hamamatsu Photonics, 812 Joko-cho, Higashi-ku, Hamamatsu, Shizuoka 431-3196, Japan*
[4]*NEC Electronics, 1753, Shimonumabe, Nakahara, Kawasaki 211-8668, Japan*
[5]*Osaka University, 2-6 Yamadaoka, Suita, Osaka 565-0871, Japan*

(Received 10 April 2009; accepted 21 April 2009; published online 13 May 2009)

We have developed a laser terahertz emission microscope utilizing excitation laser pulses at 1.06 μm wavelength for the inspection and localization of electrical failures in large-scale integrated circuits with multilayered interconnection structures. The system enables to measure terahertz emission images from the backside of a large-scale integrated circuits chip with a multilayered interconnection structure that prevents the observation from the front side. By comparing the terahertz emission images, we successfully distinguish a normal circuit from damaged ones with different positions of the interconnection defects without any electrical probing. © *2009 American Institute of Physics*. [DOI: 10.1063/1.3133346]

Imaging with terahertz wave have been seen a surge in interest and many fruitful applications such as detection of foam insulation defects,[1] illicit drug detection,[2] and package inspection[3] have been reported. Recently, a noncontact inspection technique for electrical failures in large-scale integrated circuits (LSIs) using a laser terahertz emission microscope (LTEM) has been proposed and demonstrated.[4,5] LTEM measures terahertz emission images obtained by scanning a sample with ultrafast laser pulses. The principle of the LSI inspection using LTEM is as follows. By exciting *p-n* junctions in LSIs with ultrafast laser pulses, the electric fields of the depletion layers accelerate the photoexcited carriers and the generated ultrafast transient current emits the terahertz wave. The waveform of the terahertz emission from a *p-n* junction depends on the interconnection structure that works as an antenna.[5] Therefore, comparison of the terahertz emission images between a normal chip and a defective one enables to recognize the interconnection defects that cause the change in transient photocurrent path.

Compared with conventional LSI testing methods,[6–8] this technique has various advantages. There is no need for electrical probing to check the condition of LSIs, which avoids supermultipin connections between the chip and outside equipment. Furthermore, the technique realizes the inspection of electrical failures in LSIs in which electrode pads have not yet been added during the manufacturing process. In LSI research and development, these features accelerate the improvement in the manufacturing process through failure analysis in early production stages.

Advanced LSI technology requires most LSIs to have a multilayered interconnection structure so as to allow a significant reduction in chip size. The front side of the chip is covered with metallic layers, as illustrated in Fig. 1, and prevents the photoexcitation of *p-n* junctions, which requires the observation from the backside through the silicon substrate of the chip. However, the previous setup[4,5] utilizes 800 nm wavelength femtosecond laser pulses that cannot reach to and excite *p-n* junctions through silicon substrate. In this letter, we describe an LTEM utilizing excitation laser pulses at 1 μm wavelength that allowed the successful acquisition of terahertz emission images from the backside of an LSI chip with a multilayered interconnection structure. To evaluate the inspection capability of the system, we also measured test circuits composed of silicon *p*-channel metal-oxide-semiconductor field-effect-transistors (Si *p*-MOSFETs) and identified a relationship between the terahertz emission images and the positions of disconnections along the lines connected to the *p-n* junctions.

The schematic diagram of the LTEM system for backside observation of a LSI chip is shown in Fig. 2. For the generation of the terahertz waves from the sample, we used a synchronously pumped optical parametric oscillator (OPO) excited with a mode-locked Ti:sapphire laser. The OPO produces near-infrared laser pulses: wavelength tuning range 1.0–1.3 μm, repetition rate 76 MHz, and pulse width 150 fs. The absorption coefficient of silicon strongly depends on the wavelength of the excitation laser and the doped carrier density.[9] Because the carrier density of the sample substrate was not known, we selected the wavelength so that the terahertz emission signal from the sample becomes maximum. In this experiment, the wavelength of 1.06 μm was used for the excitation of *p-n* junctions and the generation of the tera-

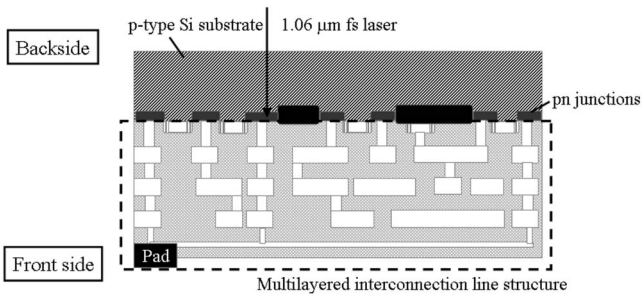

FIG. 1. Cross section of an LSI chip with multilevel interconnection lines.

[a)]Electronic mail: m-yama@riken.jp.

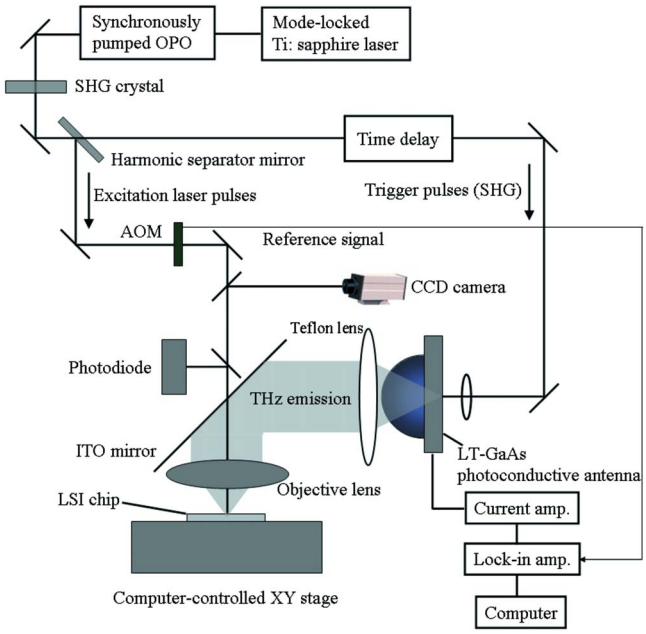

FIG. 2. (Color online) Experimental setup of the near-infrared LTEM for backside observation of LSI chips.

hertz emission through the silicon substrate of the sample. The position of the laser excitation in the LSI can be observed by a charge coupled device camera. Terahertz waves emitted through the silicon substrate of the sample are collected and focused onto a low-temperature-grown GaAs (LT-GaAs) photoconductive antenna triggered by the second harmonic (530 nm) of the OPO that increases the detection sensitivity compared with that with 1.06 μm wavelength. The signal from the detector is fed into a lock-in amplifier synchronized with the acousto-optic modulator that modulates the excitation laser at a frequency of 50 kHz. Terahertz emission images are acquired by moving the sample mounted on the computer-controlled *XY* stage with fixing the time delay stage at the peak of the terahertz waveforms. Optical images of the sample are also acquired by detecting the reflection of the excitation laser from the sample. The spatial resolution of the system is about 1.6 μm, which is limited by the excitation laser spot size at the *p-n* junctions in the sample.

In Figs. 3(a) and 3(b), we show the laser reflection image and the terahertz emission image of a test circuit in a multilayered logic LSI chip. Both images were observed from the backside of the chip without electrical contact. The image acquisition time of approximately 30 min for the image size of 6 mm^2 with 1024×1024 pixels is limited by the signal integration time of 1 ms per pixel and the speed of the computer-controlled stage. Figure 3(c) shows the waveforms of the terahertz emission from areas A and B shown in Fig. 3(d) that shows the magnified image of the area indicated by a solid square in Fig. 3(b). The polarity of the terahertz emission waveforms reflects the direction of the transient photocurrent from *p-n* junctions. The terahertz emission images were acquired by fixing the time delay at the peak indicated by an arrow in Fig. 3(c). In Fig. 3(b), the terahertz emission signal can be seen from most part of the LSI where *p-n* junctions are distributed and larger signals are observed from the edge than that from the internal part of the LSI. In Fig. 3(d), the cross-sectional distribution of the terahertz emission

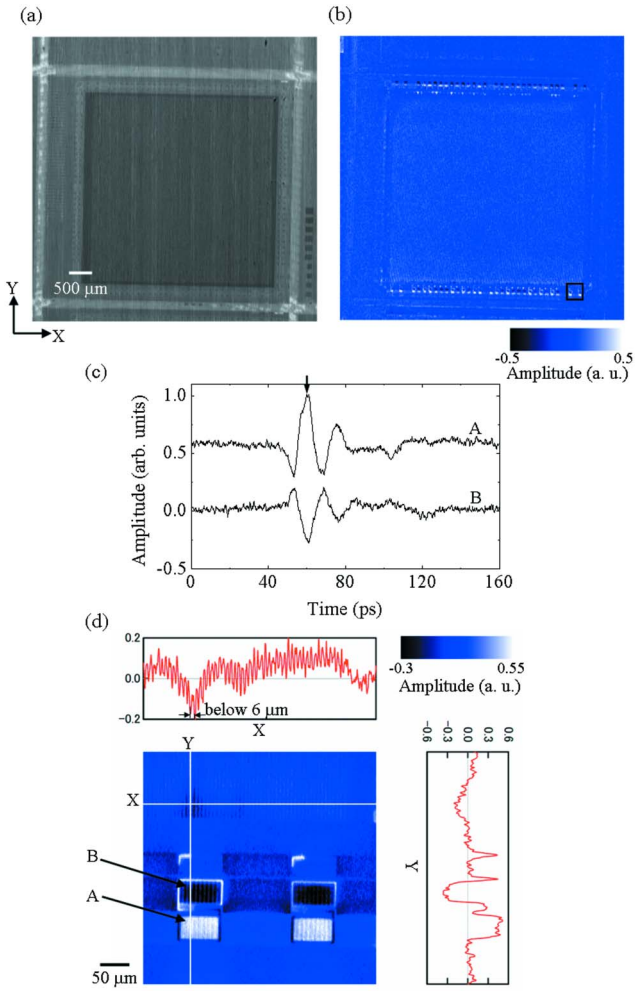

FIG. 3. (Color online) (a) Laser reflection image and (b) terahertz emission image of an LSI chip with multilayered interconnections. The size of image in (a) and (b) is approximately 6 mm^2 with 1024×1024 pixels. (c) The waveforms of terahertz emission from areas A and B in (d) the magnified terahertz emission image of the area indicated a solid square in (b). Image size is 350 μm^2 with 350×350 pixels.

in the line *X* shows the internal fine structure of a period below 6 μm. The difference of the terahertz emission signals in Fig. 3(b) is mainly attributed to the structure of the interconnection lines and *p-n* junctions in the LSI.

To elucidate the ability for the noncontact inspection of electrical failures in semiconductor devices, test circuits composed of Si *p*-MOSFETs were measured from the backside of the chip. Schematic illustrations of test circuits are shown in Fig. 4(a). In addition to the normal circuit (labeled MOSN), we prepared three defective ones (MOSD1-MOSD3) with a different position of the disconnection of the line between the heavily doped areas in *n*-type and the electrode pad, as shown by circles in Fig. 4(a). MOSD1 and MOSD2 have disconnections on the lines from both areas A and B, differing in the fact that in MOSD1 the lines are interrupted near A and B while in MOSD2 there is a single interruption near pad C. MOSD3 has a disconnection only on the line from the area B. The terahertz emission images of the test circuits from the backside of the chip are shown in Fig. 4(b). Figure 4(c) shows the waveform of the terahertz emission measured on MOSN by exciting the *p*MOSFET indicated with a white circle in Fig. 4(a). All terahertz emis-

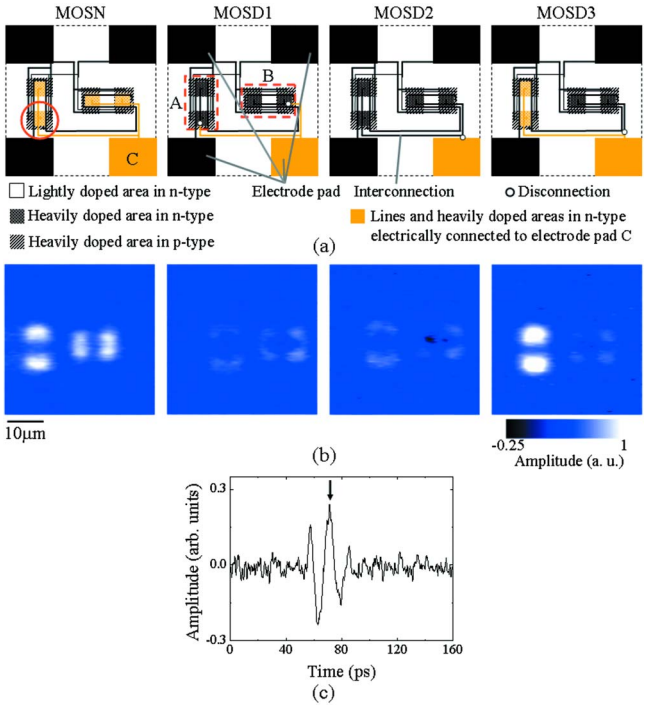

FIG. 4. (Color online) (a) Illustrations of the MOSN and the defective ones (MOSD1-MOSD3) with different disconnection positions. (b) The corresponding terahertz emission images. (c) The waveform of the terahertz emission measured by exciting the *p-n* junctions indicated by a large circle in MOSN.

sion images in Fig. 4(b) were acquired with a time delay fixed at the position indicated by an arrow in Fig. 4(c). By comparing the terahertz emission images in Fig. 4(b), one can distinguish the normal circuit from the defective ones. Furthermore, it can be seen that the terahertz emission signals from *p-n* junctions change depending on the position of the line disconnection. In MOSD1 and MOSD2, the terahertz emission signals from heavily doped areas in *n*-type in both areas A and B are smaller than that from MOSN due to the disconnection. In the case of MOSD3, the terahertz emission signals from heavily doped areas in *n*-type of A increase but that from B decrease by the disconnection between the electrode pad C and the area B, which suggests that the increase in the transient photocurrent from A flowing into the electrode pad enhances the terahertz emission signal. On the other hand, it can also be seen that there is little influence of the disconnections to the terahertz emission signals from heavily doped areas in *p*-type. These results suggest that the interconnections and electrode pad enhance the terahertz emission efficiency by working as an antenna and the change in the terahertz emission images are useful for the localization of *p-n* junctions with interconnection defects in circuits.

In summary, we have developed a LTEM using a 1 μm wavelength ultrafast laser source and successfully observed the terahertz emission image of a logic LSI chip with a multilayered interconnection from the backside of the chip. The results on test circuits reveal that the terahertz emission images of the circuits depend on the position of the disconnections and that the presence of an electrode pad and lines connected to photoexcited *p*MOSFETs enhances the terahertz emission signals. These results indicate that LTEM can be a useful tool for the inspection and localization of the open circuit defects in LSIs with multilayered interconnection without any electrical probing.

The authors would like to thank Hiroki Kitagawa for preparing the test circuits composed of Si *p*-MOSFETs. This development was supported by SENTAN, JST.

[1]N. Karpowicz, H. Zhong, J. Xu, K.-I. Lin, J.-S. Hwang, and X. C. Zhang, Semicond. Sci. Technol. **20**, S293 (2005).
[2]K. Kawase, Y. Ogawa, Y. Watanabe, and H. Inoue, Opt. Express **11**, 2549 (2003).
[3]N. Karpowicz, H. Zhong, C. Zhang, K.-I. Lin, J.-S. Hwang, J. Xu, and X. C. Zhang, Appl. Phys. Lett. **86**, 054105 (2005).
[4]T. Kiwa, M. Tonouchi, M. Yamashita, and K. Kawase, Opt. Lett. **28**, 2058 (2003).
[5]M. Yamashita, C. Otani, K. Kawase, K. Nikawa, and M. Tonouchi, Appl. Phys. Lett. **93**, 041117 (2008).
[6]K. Nikawa, Microelectron. Reliab. **37**, 1841 (1997).
[7]K. Nikawa, IEICE Trans. Electron. **E77-C**, 528 (1994).
[8]H. Fujioka and K. Nakamae, IEICE Trans. Electron. **E77-C**, 535 (1994).
[9]M. Auslender and S. Hava, *Handbook of Optical Constants of Solids* (Academic, New York, 1998), Vol. 3, p. 155.